Chinese Journal of Natural Medicines

A naturally derived small molecule compound suppresses tumor growth and metastasis in mice by relieving p53-dependent repression of CDK2/Rb signaling and the Snail-driven EMT program

Boxue REN, Yang LI, Lei DI, Ranran CHENG, Lijuan LIU, Hongmei LI, Yi LI, Zhangrui TANG, Yongming YAN, Tao LU, Rong FU, Yongxian CHENG, Zhaoqiu WU

Citation: Boxue REN, Yang LI, Lei DI, Ranran CHENG, Lijuan LIU, Hongmei LI, Yi LI, Zhangrui TANG, Yongming YAN, Tao LU, Rong FU, Yongxian CHENG, Zhaoqiu WU, A naturally derived small molecule compound suppresses tumor growth and metastasis in mice by relieving p53-dependent repression of CDK2/Rb signaling and the Snail-driven EMT program, Chinese Journal of Natural Medicines, 2024, 22(2), 1-16. doi: 10.1016/S1875-5364(24)60550-9.

View online: https://doi.org/10.1016/S1875-5364(24)60550-9

Available online at www.sciencedirect.com
ScienceDirect
Chinese Journal of Natural Medicines 2024, **22**(2): 112-126
doi: 10.1016/S1875-5364(24)60550-9
Chinese Journal of Natural Medicines

•Original article•

A naturally derived small molecule compound suppresses tumor growth and metastasis in mice by relieving p53-dependent repression of CDK2/Rb signaling and the Snail-driven EMT

REN Boxue[1Δ], LI Yang[1Δ], DI Lei[1Δ], CHENG Ranran[1Δ], LIU Lijuan[1], LI Hongmei[1], LI Yi[1], TANG Zhangrui[1], YAN Yongming[2], LU Tao[1], FU Rong[1*], CHENG Yongxian[2*], WU Zhaoqiu[1*]

[1] *State Key Laboratory of Natural Medicines, Department of Pharmacology, School of Pharmacy, China Pharmaceutical University, Nanjing 211198, China;*
[2] *Institute for Inheritance-Based Innovation of Chinese Medicine, School of Pharmaceutical Sciences, Shenzhen University Health Science Center, Shenzhen 518060, China*

Available online 20 Feb., 2024

[ABSTRACT] The tumor suppressor protein p53 is central to cancer biology, with its pathway reactivation emerging as a promising therapeutic strategy in oncology. This study introduced LZ22, a novel compound that selectively inhibits the growth, migration, and metastasis of tumor cells expressing wild-type p53, demonstrating ineffectiveness in cells devoid of p53 or those expressing mutant p53. LZ22's mechanism of action involves a high-affinity interaction with the histidine-96 pocket of the MDM2 protein. This interaction disrupted the MDM2-p53 binding, consequently stabilizing p53 by shielding it from proteasomal degradation. LZ22 impeded cell cycle progression and diminished cell proliferation by reinstating the p53-dependent suppression of the CDK2/Rb signaling pathway. Moreover, LZ22 alleviated the p53-dependent repression of Snail transcription factor expression and its consequent EMT, effectively reducing tumor cell migration and distal metastasis. Importantly, LZ22 administration in tumor-bearing mice did not manifest notable side effects. The findings position LZ22 as a structurally unique reactivator of p53, offering therapeutic promise for the management of human cancers with wild-type *TP53*.

[KEY WORDS] LZ22; Wild-type p53; p53 Reactivator; Snail-driven EMT; Tumor growth and metastasis
[CLC Number] R965 **[Document code]** A **[Article ID]** 2095-6975(2024)02-0112-15

Introduction

Cancer, a formidable challenge in extending global life expectancy, remains a critical concern [1]. In 2020, there were approximately 19.18 million new cancer cases reported worldwide. Tumor metastasis, the primary cause of mortality among cancer patients, is often linked to treatment failures due to metastatic progression [2-5]. Although metastasis is a complex process involving numerous factors and genetic events, enhanced invasion and migration are the most lethal aspects [6]. Effective cancer management requires strategies that target both tumor development, comprising tumorigenesis and metastasis, to improve clinical outcomes [7].

Ganoderma lucidum (*G. lucidum*), a traditional natural medicine, exhibits a range of pharmacological activities, including antitumor, hepatoprotective, antioxidant, and antiviral properties [8-11]. Recent research has intensified focus on *G. lucidum*, leading to the extraction of numerous aromatic heteriterpenoids. Among these, LZ22 has emerged as a unique compound with potent antitumor effects. It selectively inhibits the proliferation of tumor cells expressing wild-type p53 while sparing cells with mutant or absent p53. This

[Received on] 25-Sep.-2023
[Research funding] This work was supported by the National Natural Science Foundation of China (Nos. 82125036, 82273964, 81973363, 82304538, and 81973188), the State Key Laboratory of Natural Medicines of CPU (No. SKLNMZZ202207), the "Double-First Class" Program of CPU, the National Key Research and Development Program of China (No. 2017YFA0503900), the Jiangsu Provincial Natural Science Fund for Distinguished Young Scholar (No. BK20230042), the Jiangsu Funding Program for Excellent Postdoctoral Talent (No. 2023ZB171), and the Shenzhen Fundamental Research Program (No. JCYJ20200109114225087).
[*Corresponding author] E-mails: furong@cpu.edu.cn (FU Rong); yxcheng@szu.edu.cn (CHENG Yongxian); zqwu@cpu.edu.cn (WU Zhaoqiu)
[Δ]These authors contributed equally to this work.
These authors have no conflict of interest to declare.

discovery represents a significant advancement in the study of *G. lucidum*'s aromatic heteriterpenoids and their antitumor potential.

The tumor suppressor protein p53 is renowned for its critical biochemical properties and its pivotal role in cell homeostasis, closely correlating with tumor progression and clinical prognosis [12, 13]. Dysfunction of p53 promotes epithelial-mesenchymal transition (EMT) by activating the expression of Snail protein, thereby enhancing the migration and invasion of tumor cells. Clinically, this dysfunction manifests as increased rates of proliferation, metastasis, and recurrence [14]. Hence, p53 acts as the central hub of molecular networks to protect normal cells from cancer proliferation and tumor development by regulating biological processes such as cell cycle progression, senescence, cell metabolism, tumor microenvironment, tumor metastasis, and angiogenesis.

TP53, the gene encoding the p53 protein, is a multifunctional and highly regulated transcription factor. Deletion or mutation of p53 abolishes its function as a tumor suppressor [15]. Clinically, approximately 50% of cancer patients retain wild-type *TP53* status, and the expression of wild-type and functional p53 protein is low. However, these patients often exhibit low expression of functional p53 protein, poor p53 stability, impaired monitoring function, and consequently, a grim prognosis, frequently leading to tumor metastasis and recurrence. Therefore, improving p53 protein stability is urgently needed [16]. As a negative regulator of p53, the MDM2 protein acts as an E3 ubiquitin ligase that specifically catalyzes the degradation of p53 through the ubiquitination proteasome pathway, thereby limiting the activity of the p53 protein [17-19]. In addition, MDM2 promotes p53 export from the nucleus, preventing its DNA binding and diminishing p53 expression [20]. MDM2 has been shown to play vital roles in the tumor suppressor function of p53, and the expression of p53 was restored by blocking the interaction between MDM2 and p53, thus restoring the activity and function of wild-type p53 [21-23]. Restoring the impaired function of a single gene, p53, could provide an attractive new avenue for anticancer therapy by directly disrupting the MDM2-p53 interaction. Herein, we successfully identified a structurally novel MDM2-p53 interaction inhibitor, LZ22. LZ22 forms a high-affinity complex with the histidine-96 pocket of MDM2, remarkably disrupting the interaction of MDM2 with p53, which consequently enhances p53 stability. Our findings demonstrated that LZ22 induced p53-dependent antitumor activity, suggesting that pharmacological targeting of the p53-MDM2 interaction *via* LZ22 offers a promising therapeutic avenue for treating specific human cancers harboring wild-type *TP53*.

Materials and Methods

Cell culture

The cell lines, HCT116, MDA-MB-231, SUM159, 4T1, HT1080, DLD1, and SW620, were purchased from the American Type Culture Collection. These cell lines were cultured in Dulbecco's modified Eagle's medium (DMEM, Thermo, Waltham, MA, USA) with 10% heat-inactivated fetal bovine serum (FBS, Thermo) and 1% penicillin/streptomycin solution (KeyGEN Biotech, Nanjing, China) at 37 °C in a 5% CO_2 atmosphere. The isogenic HCT116 $p53^{-/-}$ cell line, kindly provided by Dr. B. Vogelstein (Johns Hopkins University, Baltimore, USA), was also cultured in DMEM with 10% FBS and 1% penicillin/streptomycin solution. The PyMT cancer cell line was generated in our laboratory using the method detailed in our previous study [24].

Cloning and virus production and infection

The pLKO.1-p53-shRNA vector was purchased from GenScript Biotech (Nanjing, China). Full-length cDNA of p53, tagged with GFP, was amplified by polymerase chain reaction (PCR) and subsequently cloned into the pLenti-lox vector. The vectors, pLKO.1-shRNA, psPAX2, and pMD2.G, were obtained from Addgene. Virus production and infection were performed following the previously established method [24].

Histological staining and immunohistochemistry (IHC)

Hematoxylin and eosin (H&E) and Masson's trichrome staining were performed using a kit obtained from Sigma-Aldrich (St. Louis, Missouri, US) [25]. For IHC, paraffin-embedded tumor tissues were sectioned at a thickness of 5 μm. These sections were deparaffinized with three xylene washes and rehydrated through a graded ethanol series. Antigen retrieval was achieved by heating the sections in a citric acid-based Antigen Unmasking Solution. After cooling to room temperature, the sections were permeabilized with 0.3% Triton X-100 in PBS. Endogenous peroxidase activity was quenched using 1% hydrogen peroxide in PBS. The sections were then blocked in PBS containing 1% bovine serum albumin and 5% goat serum, followed by overnight incubation at 4 °C with primary antibodies against Ki67 (Abcam, ab15580), phospho–histone H3 (CST, 9701), cleaved caspase 3 (CST, 9661), phospho-Rb, CDK2, E-cadherin, vimentin, and γH2AX. The next day, the sections were washed three times in PBS and incubated with biotin-labeled goat anti-mouse or goat anti-rabbit IgG secondary antibodies for 30 min. Horseradish peroxidase activity was detected using a standard ABC kit (Vector Laboratories) and DAB (Vector Laboratories). Finally, all selections were counterstained with hematoxylin, dehydrated, and mounted. For immunofluorescence (IF) analysis, tissue sections were incubated with primary antibodies against collagen I (Abcam, ab34710), α-SMA (Abcam, ab5694), CD45 (Biolegend, 103120), CD31 (Dianova, DIA310), and F4/80 (eBioscience, 14-4801-81), and then with goat anti-mouse and anti-rabbit Alexa Fluor secondary antibodies. All sections were counterstained with DAPI and imaged using a confocal fluorescence microscope (Zeiss LSM 800).

Statistical analysis

All the data obtained from at least five independent experiments were expressed as the mean ± SD. Statistical analyses were conducted using a one-way analysis of variance (ANOVA) or a two-sided Student's *t*-test. A P-value < 0.05 was considered statistically significant.

The details of the experimental methods employed are provided in Supplemental Methods. The sequences of all

quantitative real-time PCR (qRT-PCR) primers utilized in this study are shown in Table S1.

Results

LZ22 reduces the proliferation of tumor cells expressing wild-type p53

LZ22, an HPLC-grade pure, small-molecule aromatic compound previously isolated from *G. lucidum*, was characterized as (2*E*,4*E*)-5-(8-hydroxydibenzo[b,d]furan-4-yl)-2-methylpenta-2,4-dienal ($C_{18}H_{14}O_3$; MW 278) (Fig. 1A). To gurantee the quality including the strcuture and the purity of LZ22 used in this study, HPLC, MS, and NMR analyses were freshly conducted (Fig. S1). To determine LZ22's effect on tumor cell growth, we utilized the Cell Counting Kit-8 (CCK-8) assay across various cell lines. After 48 h of LZ22 treatment, we observed a dose-dependent decrease in the viability of tumor cells expressing wild-type p53 (human colorectal carcinoma HCT116 cells, human fibrosarcoma HT1080 cells, and mouse mammary carcinoma PyMT cells) (Fig. 1B). In striking contrast, LZ22 exhibited minimal impact on the proliferation of mutant p53-expressing tumor cells (human colorectal carcinoma DLD1 and SW620 cells and human breast carcinoma SUM159 and MDA-MB-231 cells) or tumor cells with null p53 (mouse mammary carcinoma 4T1 cells and HCT116-p53$^{-/-}$ cells, an isogenic HCT116 cell line in which both alleles of *TP53* are inactivated by homologous recombination) (Fig. 1C). These findings underscore the p53-dependent nature of LZ22's inhibitory effect on cell proliferation. To gain an unbiased insight into LZ22's overall impact on cancer cell functions, we conducted transcriptome RNA sequencing (RNA-seq) of HCT116 cells treated with either LZ22 or a control vehicle. Using a minimum threshold of a 2-fold change, we identified alterations in 1834 unique transcripts following LZ22 treatment, with 772 transcripts upregulated and 1062 downregulated (Figs. 1D−1E). Gene Ontology (GO) analysis indicated that LZ22 predominantly influenced genes within the p53 signaling pathway (with the highest RichFactor), metabolic pathways, and other carcinoma-related signaling pathways (Fig. 1F). Quantitative PCR analysis further confirmed that LZ22 treatment in HCT116

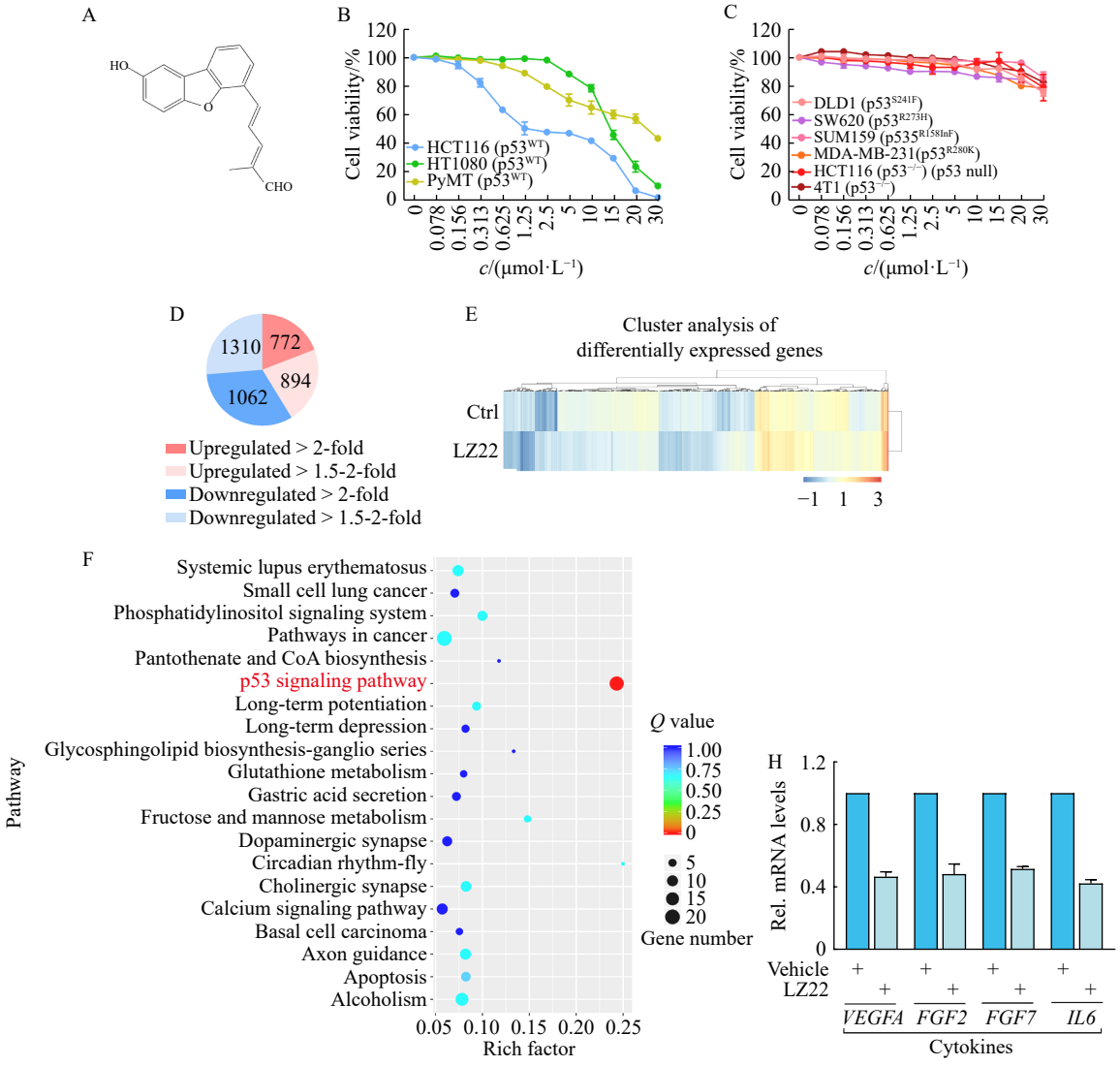

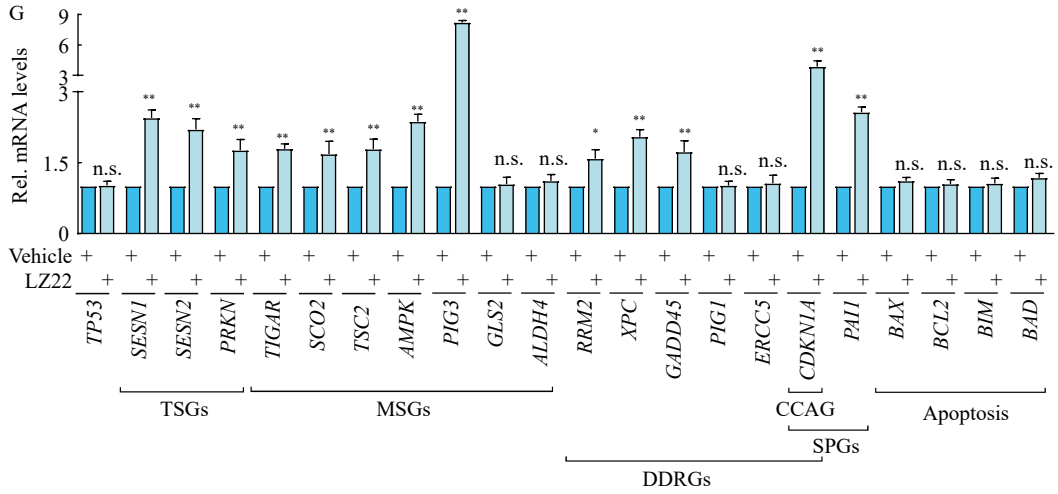

Fig. 1 LZ22 reduces the proliferation of tumor cells expressing wild-type p53 and enhances the activity of the p53 signaling pathway. (A) Structure of LZ22 extracted from *G. lucidum*. (B) CCK-8 cell proliferation assay for wild-type p53-expressing cells treated with vehicle or different concentrations of LZ22 for 48 h (n = 5). (C) CCK-8 cell proliferation assay for mutant and null p53-expressing cells treated with vehicle or different concentrations of LZ22 for 48 h (n = 5). (D−E) RNA-seq analysis of vehicle- and LZ22-treated HCT116 cells. The pie chart denotes the distribution of total transcripts changed in LZ22-treated cells compared with vehicle-treated cells (D) and the heat map of all targets in vehicle- and LZ22-treated cells (E). (F) GO analysis of signature genes that are differentially expressed in vehicle- and LZ22-treated cells, revealing significantly modulated functional pathways. (G−H) qPCR analysis validated p53-targeted genes in HCT116 cells that were treated with vehicle or 1.25 μmol·L^{-1} LZ22 for 48 h (n = 5). Data are presented as the mean ± SD (n = 5). $^{*}P < 0.05$, $^{**}P < 0.01$ *vs* vehicle (n.s., not significant). A two-tailed Student's *t*-test was used for statistical analysis.

cells did not affect *TP53* expression but significantly upregulated the expressions of the cell cycle-arresting gene (CCAG) *CDKN1A* (a gene encoding p21), DNA damage-repairing genes (DDRGs; e.g., *RRM2*, *XPC*, and *GADD45*), the senescence-promoting gene (SPG) *PAI-1*, metabolic suppressor genes (MSGs; e.g., *TIGAR*, *SCO2*, *TSC2*, *AMPK*, and *PIG3*), and tumor suppressor genes (TSGs; e.g., *SESN1*, *SESN2*, and *PRKN*), all of which are recognized as direct p53 targets (Fig. 1G). Intriguingly, p53 is known to downregulate the transcription of genes that promote angiogenesis and inflammation, including *VEGFA*, *FGF2*, *FGF7*, and *IL6* [26-29]. We observed that LZ22 treatment robustly reduced the transcript levels of the p53-targeting genes in HCT116 cells (Fig. 1H). Collectively, these results demonstrate that LZ22 activates the p53 signaling pathway, leading to the inhibition of tumor cell proliferation in cells expressing wild-type p53.

LZ22 selectively upregulates wild-type p53 protein expression

Investigating LZ22's effect on *TP53* expression revealed no significant changes, yet there was a notable enhancement in the activity of the p53 signaling pathway in HCT116 tumor cells expressing wild-type p53. This prompted an exploration into whether LZ22 influences p53 protein expression levels in tumor cells harboring wild-type or mutant *TP53* (or *Trp53*). LZ22 was observed to upregulate p53 and p21 proteins in a dose-dependent manner in cells with wild-type p53, whereas it exerted no effect on these protein levels in cells with mutant p53 (Fig. 2A and Fig. S2A). Both p53 and p21 were either undetectable or barely detectable) in HCT116-p53$^{-/-}$ or 4T1 tumor cells following LZ22 treatment (Fig. S2A). Furthermore, LZ22 treatment time-dependently increased the p53 protein levels in HCT116 and HT1080 tumor cells (Fig. 2B). In addition, LZ22-upregulated expression of p53 protein in HCT116 and HT1080 tumor cells was confirmed by IF assays (Fig. 2C). Consistent with the findings observed in HCT116 tumor cells (Fig. 1G), LZ22 failed to affect the mRNA expression of *TP53* (or *Trp53*) but did increase p53 protein levels and both the mRNA and protein levels of p21 in the other two tumor cell lines expressing wild-type p53 (Fig. 2A and Fig. S2B). Treatment with LZ22 at up to 30 μmol·L^{-1} or for up to 48 h had no impact on p53 or p21 expression at either the mRNA or protein level in mutant p53-expressing tumor cell lines (Fig. 2A, and Figs. S2A−S2B). The above findings suggest that LZ22 specifically regulates the expression of wild-type at the post-translational level. To further determine the differential regulation of LZ22 on the expression of wild-type *vs* mutant p53, we infected HCT116-p53$^{-/-}$ tumor cells with lentiviral constructs expressing GFP-tagged wild-type, R248W mutant, or R175H mutant p53, and the expression of exogenous p53 was assessed in vehicle- *vs* LZ22-treated cells. In this setup, LZ22 markedly elevated the protein level of exogenously expressed wild-type p53 but had no impact on the level of mutant p53 protein (Fig. 2D), which is consistent with the earlier observation that LZ22 preferentially upregulates endogenously expressed wild-type p53. Next, we examined whether LZ22 could affect the stability of wild-type p53 protein. To this end, vehicle- or LZ22-treated HCT116 tumor cells were cultured in the presence of cycloheximide (CHX) for different periods to block new protein synthesis, followed by the analysis of p53 expression. Post-CHX treatment, p53 protein became unstable and degraded rapidly in the vehicle-treated cells, while the protein was rel-

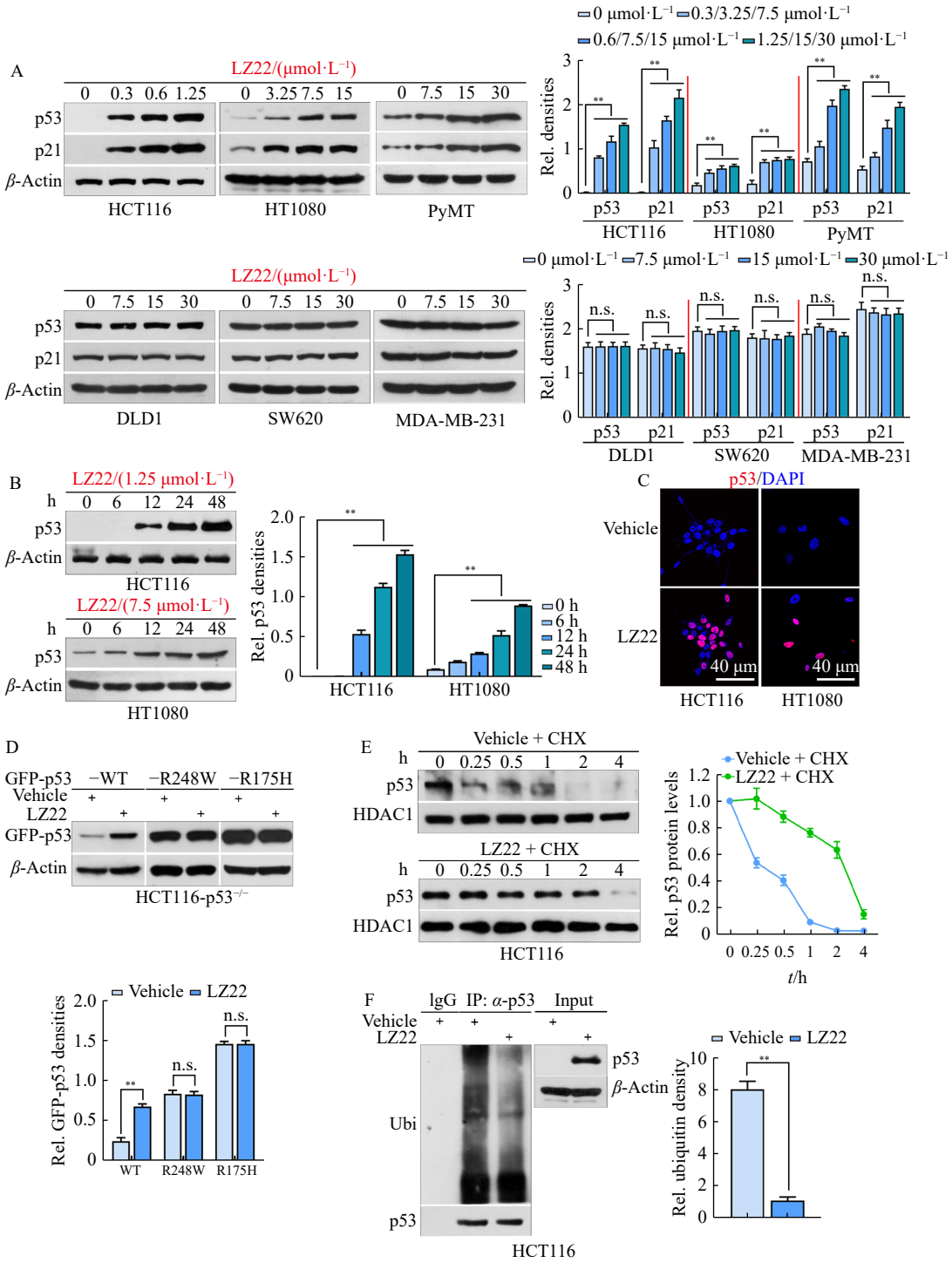

Fig. 2 LZ22 upregulates the expression of wild-type p53 through post-translation modifications. (A) Immunoblot analysis of p53 and p21 levels in various cancer cells treated with vehicle or increasing concentrations of LZ22 for 48 h. (B) Immunoblot analysis of p53 expression in wild-type p53-expressing cells treated with 1.25 μmol·L^{-1} (HCT116 cells) or 7.5 μmol·L^{-1} (HT1080 cells) LZ22 for indicated times. (C) IF staining of p53 in HCT116 (left) and HT1080 (right) cells treated with vehicle or LZ22 for 48 h. Nuclei were counterstained with DAPI (blue). (D) Immunoblot analysis of the levels of exogenous wild-type, R248W mutant, or R175H mutant p53 in HCT116-p53$^{-/-}$ cells treated with vehicle or 1.25 μmol·L^{-1} LZ22 for 48 h. (E) Immunoblot analysis of endogenous p53 expression in HCT116 cells treated with vehicle or 1.25 μmol·L^{-1} LZ22 and then with cycloheximide (CHX, 100 μg·mL^{-1}) for a total of 48 h. CHX was added to the culture medium 0.25, 0.5, 1, 2, and 4 h prior to cell harvesting, respectively. The densitometry of p53 blots is shown in the right panel. (F) Comparison of ubiquitinated endogenous p53 proteins in HCT116 cells treated with vehicle or 1.25 μmol·L^{-1} LZ22 for 48 h. MG132 (10 μmol·L^{-1}) was added 4 h before harvesting. The relative blot intensities were calculated by Image J. Data are presented as means ± SD (n = 5). $^{**}P < 0.01$ *vs* vehicle (n.s., not significant).

atively stable in the LZ22-treated cells, suggesting that LZ22 enhances the stability of p53 protein (Fig. 2E). Consistent with this observation, LZ22 remarkably decreased the ubiquitination level of endogenously expressed p53 in HCT116 tumor cells (Fig. 2F). These findings indicate that LZ22 specifically upregulates wild-type p53 at the post-translational level.

LZ22 functions as a potent MDM2-p53 binding inhibitor

Oncogenic MDM2 is a primary E3 ubiquitin ligase responsible for ubiquitination and subsequent proteasomal degradation of wild-type p53 [18], disrupting the MDM2-p53 interaction to reactivate wild-type p53 is an emerging therapeutic strategy [30]. LZ22's ability to inhibit p53 ubiquitination and enhance its stability led us to hypothesize its potential as an MDM2-p53 binding inhibitor. Molecular docking studies involving LZ22 in the MDM2 crystal structure (PDB ID: 3LBL) [31] revealed the compound forming a hydrogen bond with MDM2's evolutionarily conserved histidine-96 (H96) residue (Figs. 3A−3B). This interaction is key, as H96 is essential for MDM2's binding to p53 [31], indicating that LZ22 might disrupt this crucial interaction. Notably, LZ22 showed significantly reduced binding to the H96D mutant MDM2 protein, highlighting the critical role of the H96 residue in MDM2's interaction with LZ22 (Fig. 3C). To further assess and compare the binding interaction of LZ22 with wild-type *vs* H96D mutant MDM2 proteins, we performed an microscale thermophoresis (MST) assay to test the dissociation kinetics of LZ22. The results demonstrated that LZ22 exhibited high-affinity binding to wild-type MDM2, with a 10-fold higher affinity compared to the H96D mutant MDM2 protein (3.3 μmol·L^{-1} *vs* 33 μmol·L^{-1} in K_d) (Fig. 3D). Intriguingly, the binding interaction of compound LZ22 with p53 protein was almost completely undetectable (K_d 536 μmol·L^{-1}) (Fig. 3D). This finding was further supported by a streptavidin pulldown assay using a biotinylated derivative of LZ22 (biotin-LZ22), which confirmed the physical association of biotin-LZ22 with His-tagged MDM2 recombinant protein, but not with GST-tagged p53 recombinant protein (Figs. 3E−3F). Next, we investigated whether LZ22 could affect the binding affinity between MDM2 and p53 recombinant proteins. We observed that the binding affinity of MDM2 toward p53 in the presence of LZ22 was 192-fold lower than

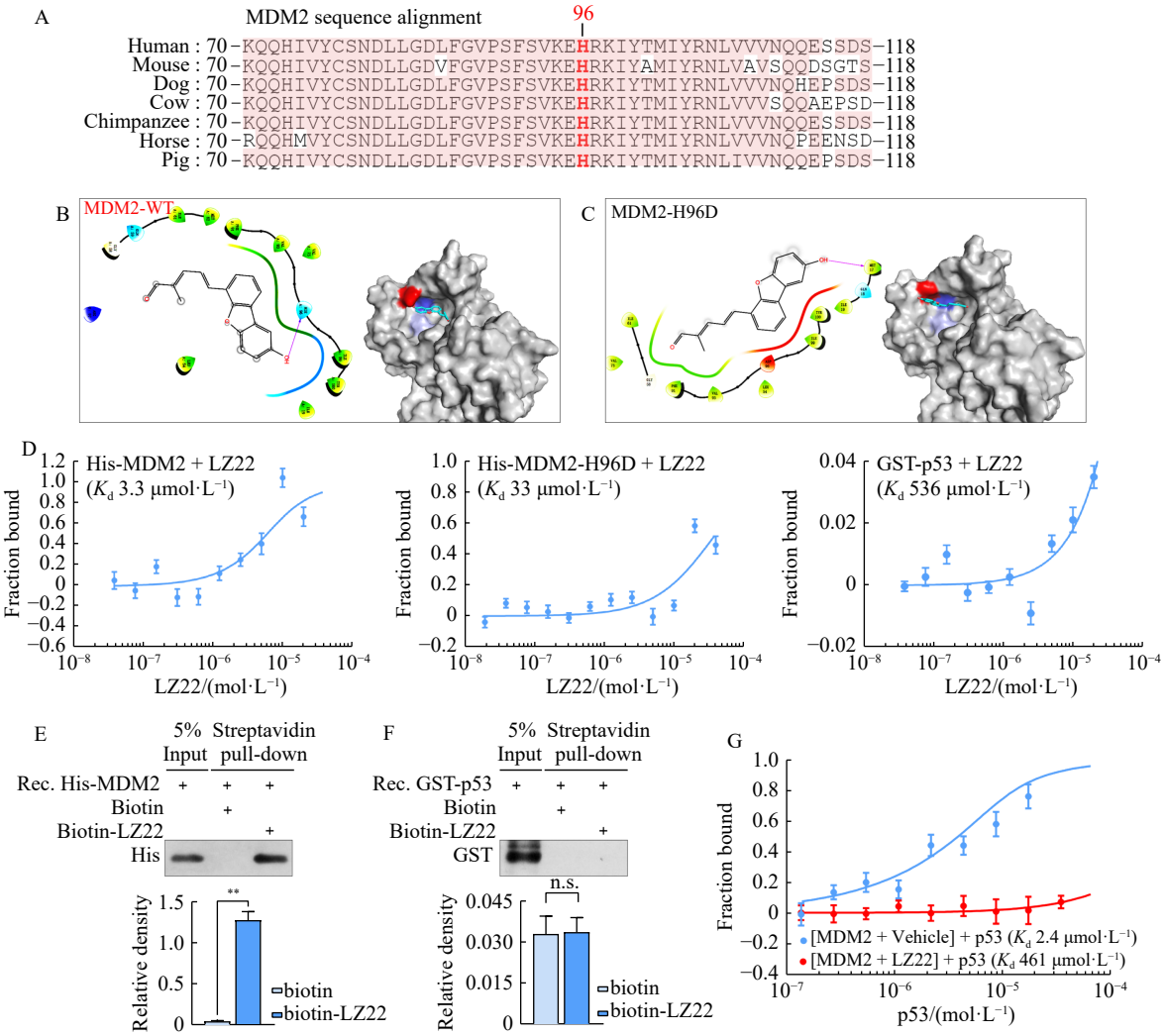

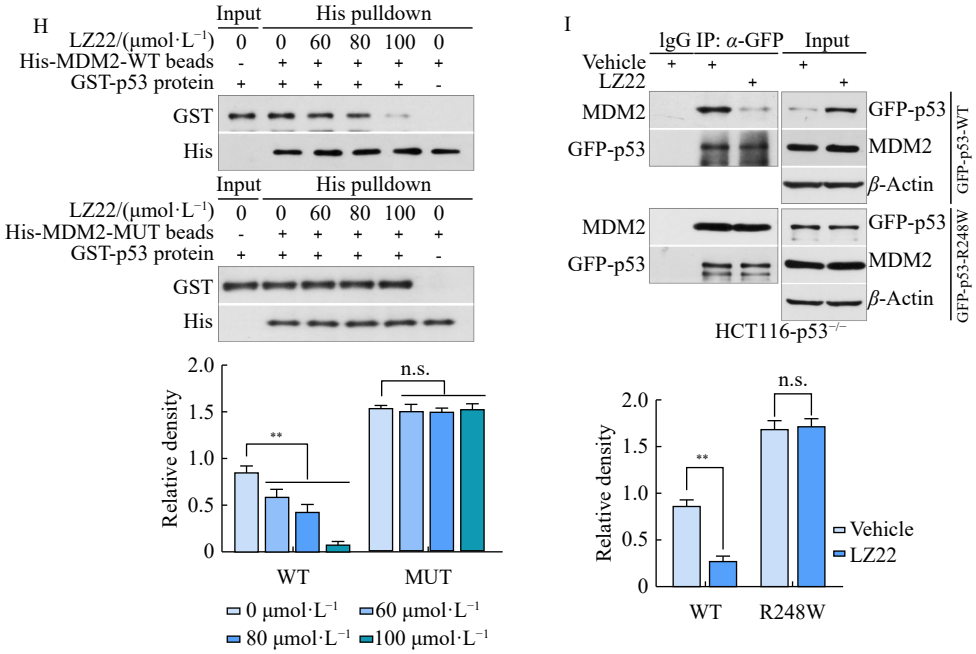

Fig. 3 LZ22 forms a high-affinity interaction with MDM2 and stabilizes p53 expression by interrupting MDM2's association with p53. (A) Diagram showing that H96 is evolutionarily conserved across species. (B−C) Molecular docking analysis of the potential binding between LZ22 and MDM2. Illustration of the surface crystal structure of LZ22 against MDM2-WT (B) and MDM2-H96D (C). (D) MST analysis of dissociation kinetics of LZ22 toward bacterially purified MDM2-WT fragment, MDM2-H96D fragment, or p53-WT. (E−F) Streptavidin pulldown assay showing that bio-LZ22 physically interacts with His-tagged MDM2 purified in *Escherichia coli* bacteria (E) without forming an interaction with bacterially purified GST-tagged p53 (F). (G) MST analysis of the dissociation kinetics of bacterially purified p53 fragment toward bacterially purified MDM2 in the presence of vehicle or LZ22. MDM2 fragment was incubated with compounds and then with the p53 fragment. (H) Recombinant His-MDM2-WT or His-MDM2-H96D proteins bound to Ni-NTA beads were co-incubated with GST-p53 protein, and the mixture was subjected to a His pulldown assay. (I) Interaction between exogenous p53 and endogenous MDM2 was monitored in cells treated with vehicle or 1.25 μmol·L^{-1} LZ22 for 48 h. The relative blot intensities were calculated by Image J. Data are presented as means ± SD (n = 5). $^{**}P < 0.01$ *vs* vehicle (n.s., not significant).

that in the absence of the compound (461 μmol·L^{-1} *vs* 2.4 μmol·L^{-1} in K_d), suggesting that LZ22 effectively impairs the binding interaction between MDM2 and p53 proteins (Fig. 3G). To further confirm that LZ22 could interrupt the binding interaction of MDM2 with p53, we used His pulldown assays in which bead-conjugated His-tagged wild-type or H96D mutant MDM2 recombinant protein was incubated with increasing concentrations of LZ22 and then with GST-tagged p53 recombinant protein. We observed that LZ22 diminished the interaction between wild-type MDM2 and p53 in a dose-dependent manner (Fig. 3H), while it had no effect on the interaction between H96D mutant MDM2 and p53 (Fig. 3H). In addition, LZ22 efficiently decreased the association of MDM2 with exogenous wild-type p53 without affecting the association of MDM2 with exogenously expressed R248W mutant p53 (Fig. 3I). Collectively, these observations suggest that LZ22 forms a high-affinity interaction with the H96 pocket of the MDM2 protein, potentially disrupting the MDM2-p53 interaction and thereby stabilizing p53 expression.

LZ22 hinders cell cycle progression by recovering p53-dependent repression of CDK2/Rb signaling in tumor cells expressing wild-type p53

To understand LZ22's long-term effects on tumor growth, we extended our initial investigation, which utilized the CCK-8 assay for a 48-h treatment period. For this, tumor cells were incubated with vehicle or LZ22 for ten consecutive days and then subjected to colony formation analysis. It was observed that LZ22 notably reduced colony formation in a dose-dependent manner in HCT116 and HT1080 tumor cells (Figs. 4A and S3A), whereas DLD1 or HCT116-p53$^{-/-}$ tumor cells displayed no significant change in colony formation capacity (Figs. 4B and S3B). Similarly, LZ22 dose-dependently diminished the colony formation capacities of control HT1080 tumor cells but did not affect the capacities of p53-silenced tumor cells (Figs. 4C and S3C), indicating that LZ22 reduces tumor cell growth by specifically stabilizing wild-type p53 protein. We next sought to identify the underlying mechanism by which LZ22 inhibits tumor cell growth. An apoptosis detection assay revealed that LZ22 did not induce the apoptosis of tumor cells with different p53 expression statuses, suggesting that the compound has no impact on tumor cell survival (Figs. S3D and S3E). Therefore, our investigation shifted focus to the influence of LZ22 on cell cycle progression. In this study, tumor cells were incubated with either LZ22 or a suitable vehicle control. Concurrently, the cells were treated with nocodazole, a microtubule-destabilizing agent, or its corresponding vehicle. Post-treat-

ment, the cells underwent fluorescence-activated cell sorting (FACS) analysis to meticulously evaluate the impact of LZ22 on their cell cycle dynamics. The results revealed that LZ22 induced G_1-phase cell cycle arrest in HCT116 and HT1080 tumor cells but not in HCT116-p53$^{-/-}$ or DLD1 tumor cells (Fig. 4D). More strikingly, most vehicle-treated HCT116 and HT1080 tumor cells entered S/G_2/M phases in the presence of nocodazole, while a large fraction of LZ22-treated cells were still arrested in G_1 phase (Fig. 4D). In contrast, compound LZ22 had no obvious impact on the cell cycle progression of DLD1 or HCT116-p53$^{-/-}$ tumor cells in the absence or presence of nocodazole (Fig. 4E). Our findings indicate that LZ22 induces G_1-phase cell cycle arrest, thus impairing tumor cell proliferation. The G_1-to-S phase transition is a critical cell cycle checkpoint, particularly in the regulation of tumor cell growth [32]. Induced by wild-type p53, the p21 protein encoded by *CDKN1A* inhibits the cyclin-dependent kinase 2 (CDK2)-cyclin E complex, resulting in decreased Rb phosphorylation and fostering the formation of the Rb-E2F complex, consequently resulting in G_1 phase arrest [33]. We next sought to assess whether LZ22 has an effect on the expression of the key molecules that drive cells from G_1 to S phase. It was found that the treatment of HCT116 and HT1080 tumor cells with LZ22 upregulated the protein expressions of p53 and p21, in tandem with marked decreases in the expression of key molecules involved in the G_1-to-S transition, including CDK2, cyclin E, and phospho-Rb (Fig. 4F). As expected, LZ22 had no impact on the expression of these key molecules in HCT116-p53$^{-/-}$ tumor cells (Fig. 4G). Considering that the p53 signaling pathway plays an important role in inducing senescence and thereby impairs tumor cell growth [34], we examined LZ22's potential to induce senescence

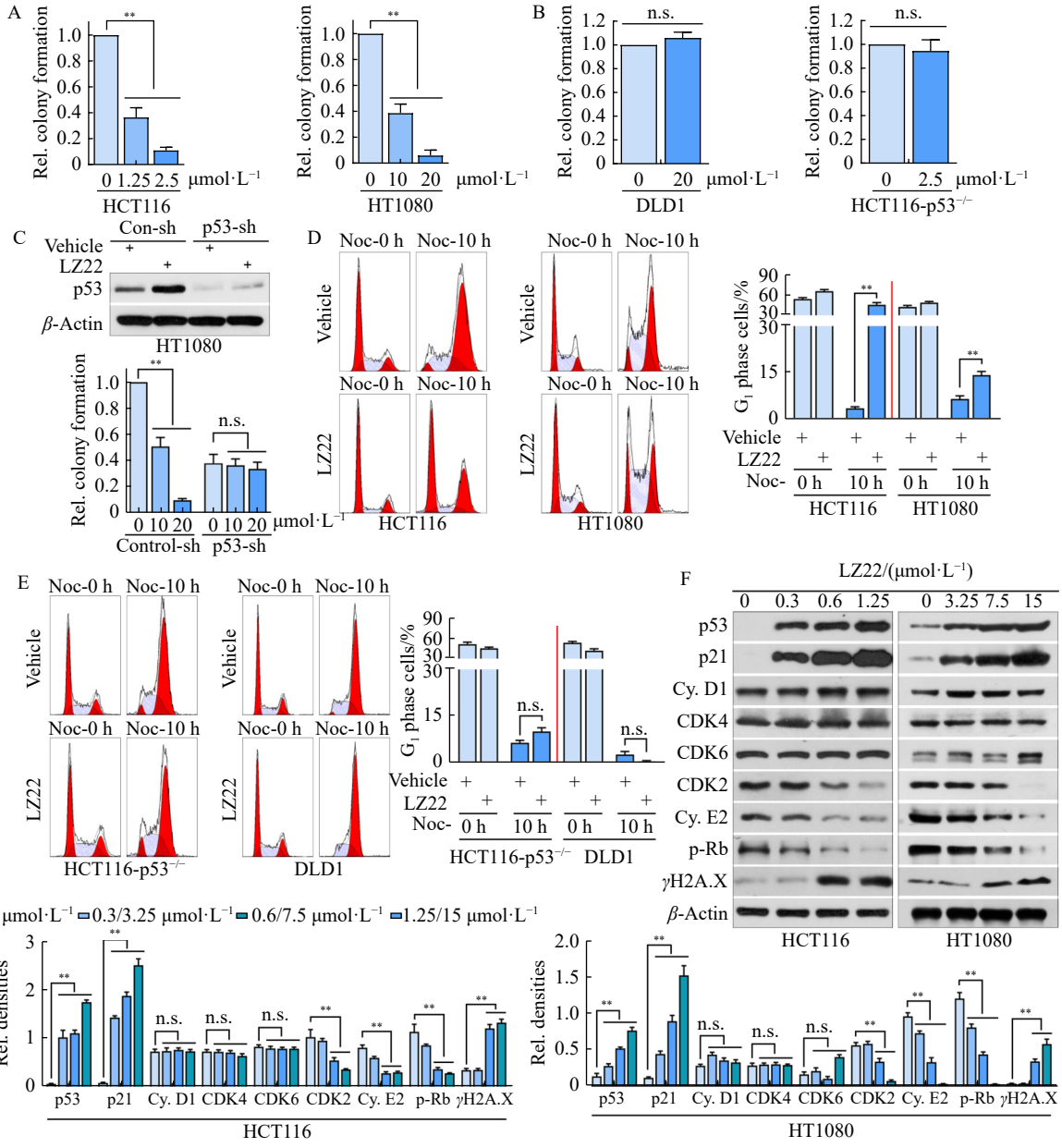

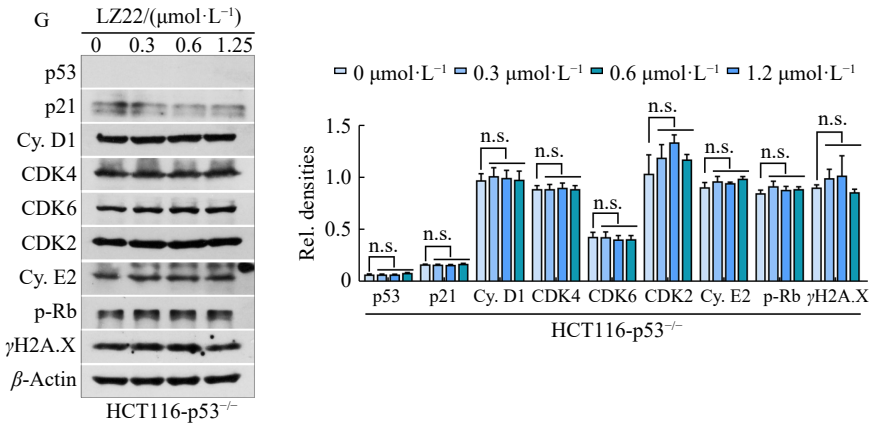

Fig. 4 LZ22 suppresses cell proliferation by recovering p53-dependent repression of CDK2/Rb signaling in tumor cells expressing wild-type p53. (A−B) Colony formation assay for wild-type (A), mutant, and null p53-expressing (B) cells treated with vehicle or different concentrations of LZ22 for ten consecutive days. (C) Immunoblot analysis of the p53 protein expression in control and p53-silenced HT1080 cells treated with vehicle or LZ22 for 48 h. Colony formation assay of control or p53-silenced HT1080 cells that were treated with vehicle or increasing concentrations of LZ22 for 10 consecutive days. (D) Cell cycle distribution of wild-type p53-expressing cells was determined by flow cytometry after treatment with vehicle or LZ22 [(1.25 μmol·L^{-1} LZ22, HCT116 cells) or (7.5 μmol·L^{-1} LZ22, HT1080 cells)] for 48 h, and nocodazole (Noc, 400 ng·mL^{-1}) was added 10 h before cell harvesting. (E) Flow cytometric analysis for cell cycle progression in mutant and null p53-expressing cells treated with vehicle or LZ22 [(1.25 μmol·L^{-1} LZ22, HCT116-p53$^{-/-}$ cells) or (30 μmol·L^{-1} LZ22, DLD1 cells)] and then with nocodazole for 10 h (48 h in total). (F) Immunoblot analysis for evaluating the impact of LZ22 with increasing concentrations on expression of p53, p21, cyclin D1, CDK4, CDK6, CDK2, cyclin E2, phospho-Rb, and γH2AX in HCT116 and HT1080 cells. (G) Immunoblot analysis of the indicated protein expression in HCT116-p53$^{-/-}$ cells treated with vehicle or increasing concentrations of LZ22 for 48 h. The relative blot intensities were calculated by Image J. Data are presented as means ± SD (n = 5). $^{**}P < 0.01$ *vs* vehicle (n.s., not significant). One-way analysis of variance (A and C) and two-tailed Student's *t*-test (B, D, and E) were used for statistical analysis.

in tumor cells with different p53 expression statuses. Using the senescence-associated β-galactosidase (SA-β-Gal) staining assay, we observed that LZ22 induced senescence in HCT116 tumor cells but not in HCT116-p53$^{-/-}$ or DLD1 cells (Fig. S3F). IF analysis further revealed that LZ22 effectively elevated the expression of the senescence marker γH2AX in HCT116 and HT1080 tumor cells without affecting its expression in HCT116-p53$^{-/-}$ or DLD1 tumor cells (Fig. S3G).

LZ22 inhibits the in vitro migration of tumor cells by recovering p53-dependent repression of Snail and the Snail-driven EMT

The tumor suppressor protein p53 is integral in impeding tumor cell EMT and migration by downregulating the Snail protein expression and activity [14]. This study explored LZ22's potential to modulate EMT and migration of tumor cells. RNA-seq and RT-qPCR analyses revealed that LZ22 treatment markedly decreased the expression of mesenchymal markers (*VIM*, *FN*, and *CDH2*) and increased the epithelial marker *CDH1* in HCT116 cells (Figs. 1E and 5A). Furthermore, LZ22-treated HCT116 tumor cells displayed a significant reduction in Snail protein expression levels, accompanied by an increase in E-cadherin and a decrease in vimentin, indicating inhibition of EMT in the cells (Fig. 5B). In striking contrast, LZ22 treatment did not change the protein expression levels of Snail, E-cadherin, and vimentin in HCT116-p53$^{-/-}$ tumor cells (Fig. 5B). The recovery of p53-dependent repression of Snail protein expression by LZ22 in HCT116 but not in HCT116-p53$^{-/-}$ tumor cells was further confirmed by IF analysis (Fig. 5C). Given the established connection between the Snail-driven EMT and tumor cell migration, we next assessed the impact of LZ22 on tumor cell migration *in vitro*. As expected, LZ22 dose-dependently reduced the migration of HCT116 and HT1080 tumor cells, concurrent with a decrease in Snail protein expression, whereas the compound did not suppress the migration of HCT116-p53$^{-/-}$ or DLD1 tumor cells (Figs. 5D and 5E). To ensure that the observed reduction in cell migration was not a consequence of decreased cell proliferation, we conducted additional experiments with cells pre-treated with LZ22 and then cultured in upper inserts with a 1-μm pore size (as opposed to the standard 8-μm pore size). This approach confirmed that cells were unable to invade the bottom well, and the proliferation of LZ22-pre-treated cells remained comparable to that of vehicle-pre-treated cells (Figs. S4A and S4B). Collectively, these findings suggest that LZ22 inhibits tumor cell migration by reactivating the p53-dependent repression of Snail protein expression and the Snail-driven EMT in tumor cells expressing wild-type p53.

LZ22 suppresses the growth and hepatic metastasis of xenograft tumors expressing wild-type p53

Next, we assessed the impact of LZ22 on the *in vivo* growth of tumor cells using a xenograft model. After 14 days of treatment, LZ22 dose-dependently inhibited HCT116 xenograft tumor growth (Fig. 6A) without eliciting toxicity in tumor-bearing mice (Figs. S5A and S5B). Immunoblot analyses revealed a significant upregulation of p53 and p21 expressions in tumors treated with LZ22 (Fig. 6B). Further, immunohistochemical experiments showed an increased num-

ber of p53$^+$ tumor cells and concomitant decreases in Ki67$^+$ (proliferative), phospho-histone H3$^+$ (mitotic), CDK2$^+$, and phospho-Rb$^+$ tumor cells following LZ22 treatment (Figs. 6C and 6D). Moreover, the number of cleaved caspase 3$^+$ (apoptotic) cells in the LZ22-treated xenograft tumors was comparable to that of the vehicle-treated tumors, suggesting that LZ22 does not induce apoptosis in xenograft tumors (Fig. S5C). The p53 protein has also been shown to play a vital role in modifying the tumor microenvironment, thereby precisely controlling tumor growth and progression [26, 35]. The influence of LZ22 on the tumor microenvironment, which is critical in tumor growth and progression, was also investigated. LZ22 treatment led to a marked reduction in the deposition of type I collagen-positive extracellular matrix (ECM) and significantly attenuated the infiltration of CD31-positive endothelial cells and α-SMA-positive tumor-associated fibroblasts (Fig. 6E). In line with the *in vitro* observations, LZ22-treated tumors exhibited reduced Snail expression and impaired EMT, as evidenced by increased E-cadherin levels and decreased vimentin levels (Fig. 6F). Next, the impact of LZ22 on tumor metastasis was further assessed using a hepatic metastasis model, which was established by intrasplenically injecting 2 × 10^6 GFP-labeled HCT116 tumor cells into nude mice. The results demonstrated that LZ22 dramatically reduced hepatic metastasis and nodule formation (Fig. 6G). These findings suggest that LZ22 is a potent inhibitor of the *in vivo* tumor growth and hepatic metastasis in xenograft models expressing wild-type p53.

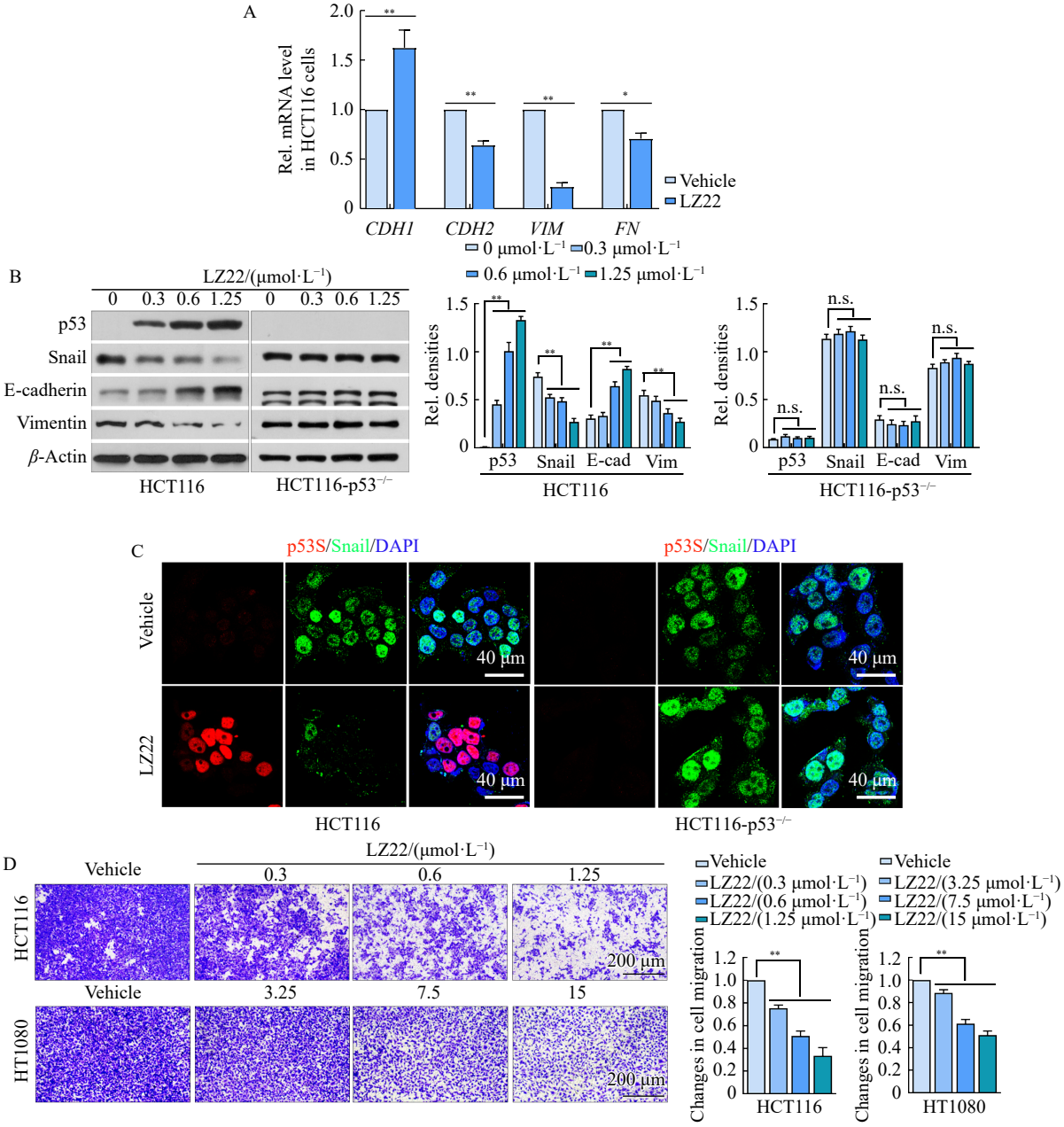

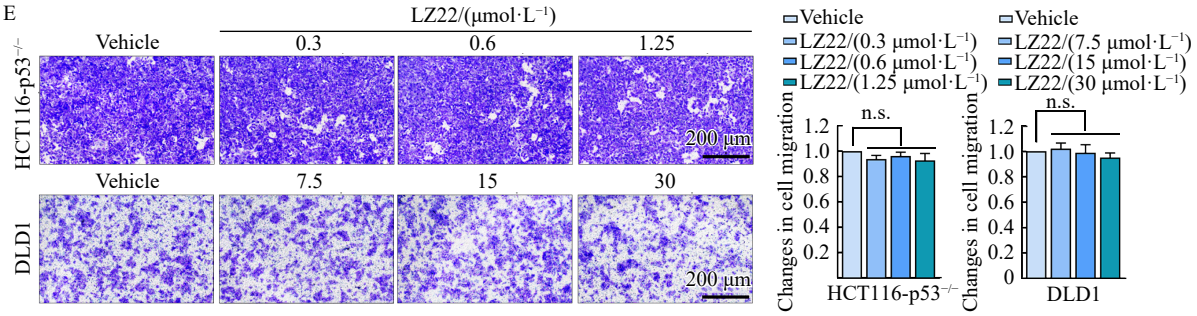

Fig. 5 LZ22 inhibits tumor migration *via* impeding Snail-driven EMT following recovering p53-dependent repression of Snail. (A) RT-qPCR analysis of *CDH1*, *VIM*, *CDH2*, and *FN1* expression in HCT116 cells treated with vehicle or 1.25 μmol·L^{-1} LZ22 for 48 h. (B) Immunoblot analysis for evaluating the impact of LZ22 with increasing concentrations on expression of p53, Snail, as well as EMT-associated markers in HCT116 and HCT116-p53$^{-/-}$ cells. (C) IF staining of p53 and Snail in HCT116 (left) and HCT116-p53$^{-/-}$ (right) cells that were treated with vehicle or 1.25 μmol·L^{-1} LZ22 for 48 h. Nuclei were counterstained with DAPI (blue). (D and E) Migration assay of wild-type (D), mutant, and null p53-expressing (E) cells that were treated with vehicle or increasing concentrations of LZ22 for 48 h. The relative blot intensities were calculated by Image J. Data are presented as means ± SD (n = 5). $^{*}P$ < 0.05 and $^{**}P$ < 0.01 *vs* vehicle (n.s., not significant). Two-tailed Student's *t*-test (A) and one-way analysis of variance (D and E) were used for statistical analysis.

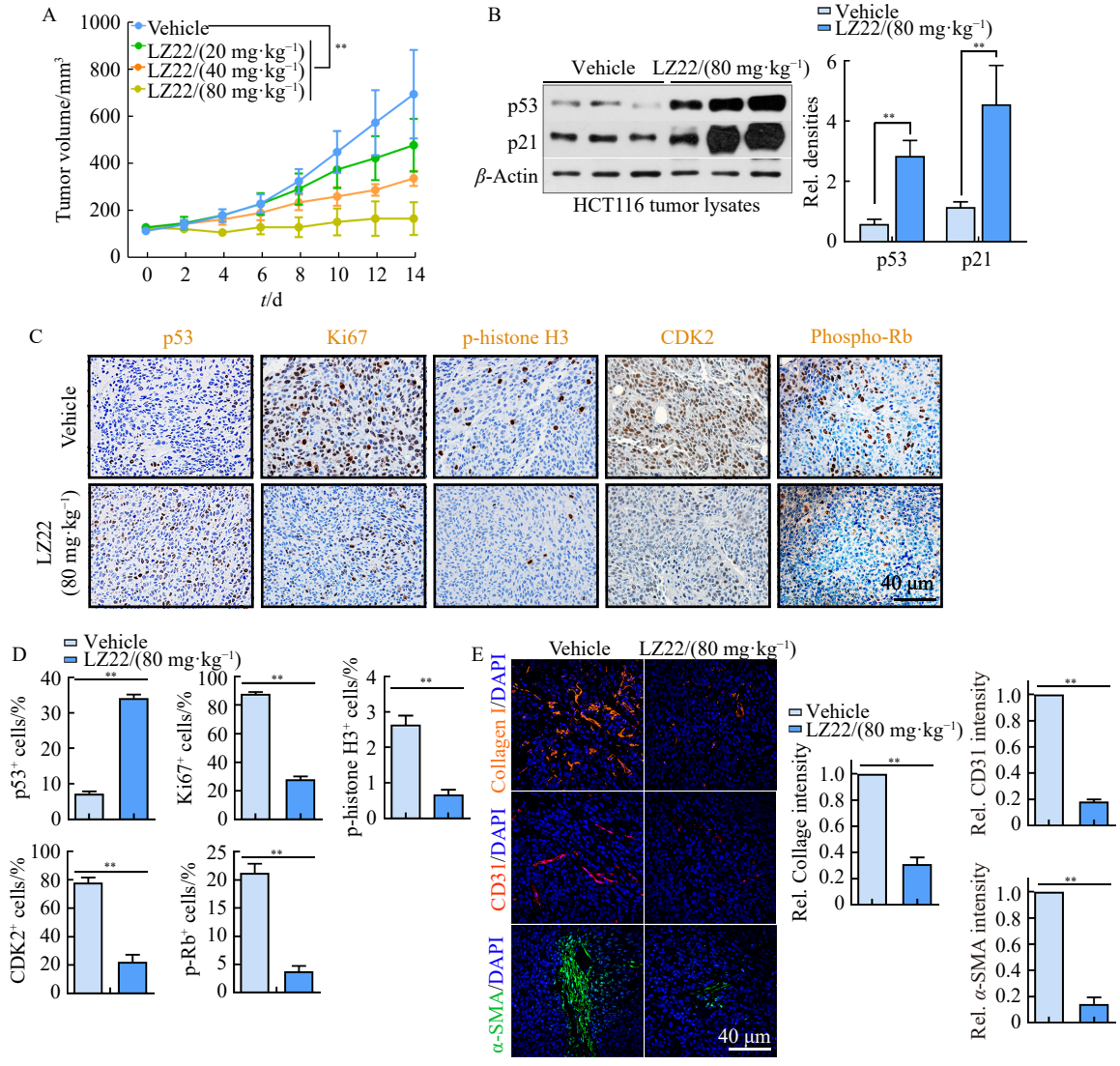

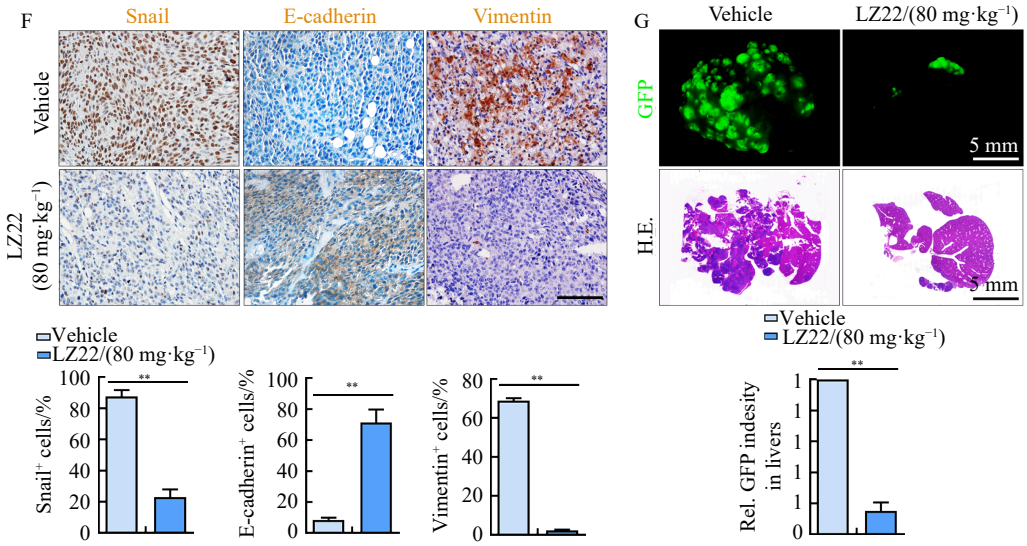

Fig. 6 LZ22 suppresses tumor growth and hepatic metastasis in colon cancer xenografts expressing wild-type p53. (A) Dose-dependent inhibition of LZ22 on the volumes of HCT116 xenograft tumors (n = 5). (B) Immunoblot analysis of p53 and p21 expression in tumor lysates of vehicle- and LZ22-treated mice (n = 5). (C) IHC of p53, Ki67, phospho-histone H3, CDK2, and phospho-Rb in vehicle- and LZ22-treated xenograft tumors (n = 5). (D) Quantification of p53$^+$, Ki67$^+$, phospho-histone H3$^+$, CDK2$^+$, and phospho-Rb$^+$ cells in tumors as described in (C). (E) IF staining of Collagen I, CD31, and α-SMA in vehicle- and LZ22-treated xenograft tumors (n = 5). Nuclei were DAPI stained. Quantification of staining intensity in xenograft tumors is shown in the right panel. (F) IHC of Snail, E-cadherin, and vimentin expression in HCT116 xenograft tumors (n = 5). Quantification of staining positive cells is shown in the bottom panel. (G) Representative phase GFP fluorescence (top) and H&E (bottom) images of vehicle- and LZ22-treated livers (n = 5). Mice were intrasplenically injected with GFP-labelled HCT116 cells and treated with vehicle or 100 mg·kg^{-1} LZ22 for three consecutive weeks, and the livers were dissected for analysis. The relative blot intensities were calculated by Image J. Data are presented as means ± SD (n = 5). $^{**}P < 0.01$ *vs* vehicle. A two-tailed Student's *t*-test was used for statistical analysis.

Consistent with the *in vitro* observations that LZ22 had no impact on the growth of mutant p53-expressing tumor cells, we observed a similar trend *in vivo*. LZ22 administration had no effect on the growth of DLD1 xenograft tumors, which harbored mutant p53 (Fig. S6A). As expected, the number of p53$^+$, Ki67$^+$, phospho-histone H3$^+$, or cleaved caspase 3$^+$ tumor cells in the LZ22-treated xenograft tumors was comparable to that in the vehicle-treated tumors (Fig. S6B). Moreover, the infiltration of CD31-positive endothelial cells and α-SMA-positive tumor-associated fibroblasts remained largely unchanged in the LZ22-treated xenograft tumors compared with that in the vehicle-treated tumors (Fig. S6C).

LZ22 reduces mammary tumor growth and pulmonary metastasis in MMTV-PyMT transgenic mice

The role of wild-type p53 in suppressing mammary tumor growth and distal metastasis is well-established in the MMTV-PyMT transgenic mouse model [26], which closely resembles human luminal B breast tumors [26]. Here, we investigated the efficacy of LZ22 on mammary tumors expressing wild-type p53 in PyMT mice. Two-month-old female mice with littermates that developed palpable breast tumors of about 0.4 cm^3 received vehicle or LZ22 treatment for four consecutive weeks, and the growth and pulmonary metastasis of mammary tumors were monitored. The results manifested that LZ22 administration significantly reduced mammary tumor growth (Fig. 7A) without causing toxicity in PyMT mice (Figs. S7A and S7B). Immunohistochemical experiments revealed an increase in p53-positive cells and a decrease in markers of proliferation and cell cycle progression, such as phospho-histone H3, Ki67, phospho-Rb, and CDK2, in LZ22-treated mammary primary tumors (Figs. 7B and 7C). Interestingly, the number of apoptotic cells in LZ22-treated mammary tumors was comparable to that in the vehicle-treated tumors (Fig. S7C). Further histological assessments, including Masson's trichrome staining and IF staining, revealed significantly reduced deposition of ECM in LZ22-treated mammary tumors compared with that in vehicle-treated tumors (Fig. 7D). The impact of LZ22 on the recruitment of tumor stromal cells was also assessed. LZ22 also effectively reduced the infiltration of CD31-positive endothelial cells and α-SMA-positive tumor-associated fibroblasts (Fig. 7E), as well as the recruitment of CD45-positive leukocytes and F4/80-positive macrophages (Fig. 7F). These findings suggest that LZ22 contributes to creating a suppressive microenvironment that may play a part in curtailing mammary tumor growth. In alignment with its proposed mechanism of action, LZ22-treated mammary primary tumors exhibited an increase in E-cadherin levels and a decrease in vimentin levels, indicating effective inhibition of the EMT *in vivo* (Fig. 7G). Consequently, LZ22 markedly reduced the number of metastatic nodules in the lungs of the treated mice (Fig. 7H).

Discussion

Over half of human malignancies harbor wild-type p53 alleles. p53, a transcription factor, is subject to stabilization

and activation by diverse genotoxic and cellular stressors, culminating in senescence, cell cycle arrest, apoptosis, and metabolic adaptation [12, 36]. The deletion and mutation of the *TP53* gene compromise its critical tumor suppressive functionality [16]. Therefore, therapies targeting wild-type p53 are at the forefront of cancer treatment research. Current p53-targeted strategies encompass various approaches: re-establishing wild-type functionality in mutant p53, restoring p53 function through gene therapy, inhibiting the p53-MDM2 interaction, targeting proteins in the p53 family, eliminating mutant p53, and leveraging p53-centric vaccines [36]. Here, we identified a novel small molecule, LZ22, derived from *G. lucidum*, which remarkably inhibited the growth, migration, and metastasis of tumor cells expressing wild-type p53 while exhibiting no significant effect on p53-deficient or mutant p53-expressing tumor cells. We further observed that LZ22 engaged in a high-affinity interaction with the H96 pocket of the MDM2 protein through its aldehyde group. Subsequent mutation of MDM2's 96th amino acid to H96D did not significantly alter the structural integrity of the protein's binding pocket. Through molecular docking analyses, LZ22 was predicted to inadequately fit within the active site of the mutated protein, causing notable compound deviation. This prediction was corroborated by microscale thermophoresis (MST) findings. It is well-established that MDM2 serves as the predominant endogenous inhibitor of wild-type p53, primarily functioning as a p53-specific ubiquitin ligase by interacting with p53's *N*-terminal transactivation domain, interrupting the MDM2-p53 binding interaction to restore the expression and activity of wild-type p53. Our findings suggest that LZ22's high-affinity binding to MDM2's H96 pocket may disrupt the MDM2-p53 interaction, thereby stabilizing and enhancing p53 expression.

The functional abrogation of p53 is a well-established factor contributing to cancer cell proliferation, primarily by disrupting cell cycle checkpoints [37]. The protein p21, a direct downstream effector of p53, is pivotal in this context. Activation of p53 markedly upregulates p21 transcription, which subsequently inhibits the CDK2-cyclin E complex. This inhibition effectively hinders RB phosphorylation, facilitating the formation of the Rb-E2F complex. As a result, this cascade arrests cell cycle progression from G_1 to S phase [33, 37]. In this study, we determined that LZ22 increased the expression of the p53-inducible tumor suppressor protein p21 and then decreased CDK2, cyclin E2, and p-Rb, thereby arresting cells through G_1 into S phase. Notably, LZ22 did not exhibit any significant effect on the cell cycle or the expression of proteins associated with the G_1 phase checkpoint in HCT116-p53$^{-/-}$ tumor cells. This finding underscores our conclusion that LZ22 induces G_1 phase cell cycle arrest by activating wild-type p53. Recent advancements in CDK4/6 inhibitors have shown promising clinical results; however, the challenge of adaptive and intrinsic drug resistance remains a sig-

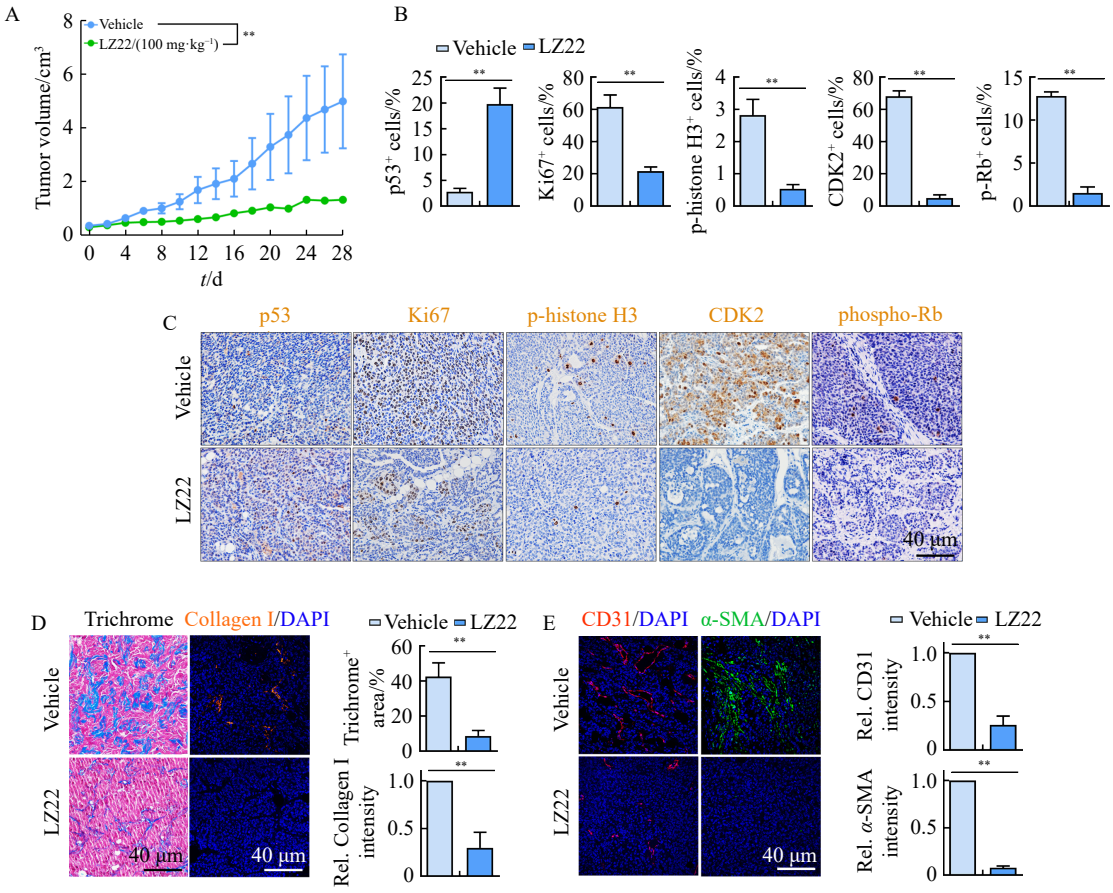

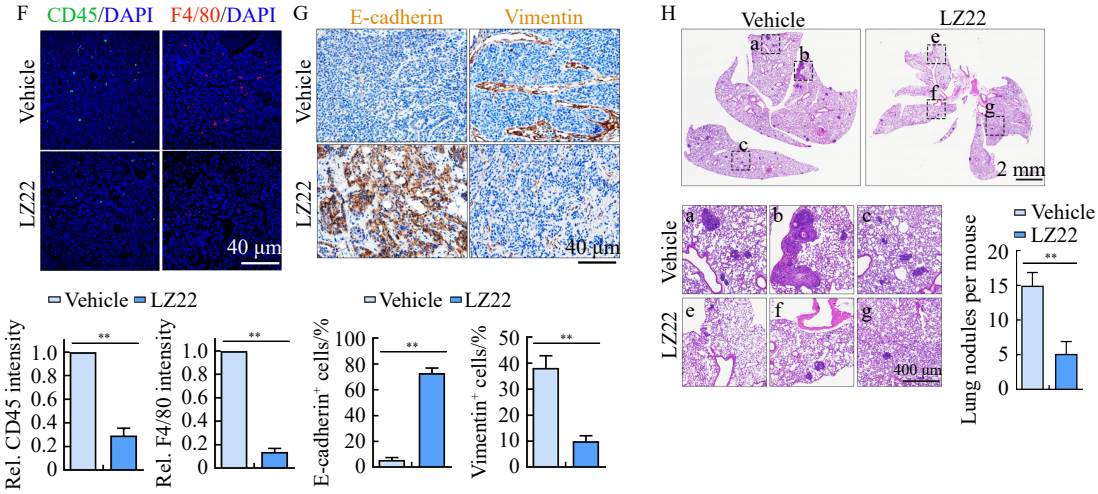

Fig. 7 LZ22 impedes PyMT mammary tumor growth and reduces spontaneous metastases. (A) Primary tumor volumes were measured in MMTV-PyMT mice that were intraperitoneally treated with vehicle or LZ22 (100 mg·kg^{-1}) for 28 consecutive days (n = 5). (B) Quantification of p53$^+$, Ki67$^+$, phospho-histone H3$^+$, CDK2$^+$, and phospho-Rb$^+$ in tumors as described in (C). (C) IHC of p53, Ki67, phospho-histone H3, CDK2, and phospho-Rb in primary tumors of vehicle- and LZ22-treated mice (n = 5). (D) Masson staining (left) and type I collagen IF staining (right) of primary tumors from vehicle or LZ22-treated mice (n = 5). Nuclei were DAPI stained. Quantification of staining intensity in primary tumors is shown in the right panel. (E) IF staining of CD31 and α-SMA in primary tumors of vehicle- and LZ22-treated mice (n = 5). Nuclei were DAPI stained. Quantification of staining intensity in primary tumors are shown in right panel. (F) IF analyses of CD45 and F4/80 in primary tumors of the indicated mice (n = 5). Nuclei were DAPI stained. Quantification of staining intensity in primary tumors are shown in bottom panel. (G) IHC of E-cadherin and vimentin expression in primary tumors (n = 5). Quantification of staining positive cells in primary tumors is shown in the bottom panel. (H) Representative H&E staining of lungs dissected from vehicle- or LZ22-treated PyMT transgenic mice (n = 5). Magnified areas of boxed sections are shown in the left panel. Quantification of nodules in vehicle- and LZ22-treated lungs are shown in the right panel. The relative blot intensities were calculated by Image J. Data are presented as means ± SD (n = 5). $^{**}P < 0.01$ *vs* vehicle. A two-tailed Student's t-test was used for statistical analysis.

nificant barrier to their long-term efficacy [38]. Research indicates that resistance to the CDK4/6 inhibitor, palbociclib, is often associated with the dysregulated activation of cyclin E/CDK2 [39]. In this context, our study revealed that LZ22 significantly elevated p53 and p21 expressions in a manner dependent on wild-type p53, thereby effectively inhibiting CDK2/Rb signaling. This inhibition leads to a marked reduction in the proliferation and metastasis of tumor cells expressing wild-type p53, all while demonstrating a favorable safety profile in tumor-bearing mice. These observations suggest that LZ22 holds potential for use in combination with CDK4/6 inhibitors, potentially enhancing their efficacy and delaying the onset of drug resistance, especially in the treatment of advanced cancers. This hypothesis presents an intriguing avenue for further research and warrants in-depth investigation.

Cisplatin is a cornerstone chemotherapy agent in the treatment of a variety of solid tumors. However, its clinical efficacy is often undermined by the emergence of acquired drug resistance and adverse effects [40, 41]. A key factor contributing to chemotherapy resistance and tumor metastasis is the EMT, a process intimately linked with tumor progression. The tumor suppressor protein p53 plays a pivotal role in mitigating tumor cell EMT and migration by inhibiting the expression and activity of the Snail protein [14]. Our research revealed that LZ22 impeded the migration of tumor cells by recovering p53-dependent repression of Snail and the Snail-driven EMT. *In vivo* experiments revealed the efficacy of LZ22 in suppressing tumor progression without eliciting notable toxic side effects in tumor-bearing mice. In light of the substantial toxicity and resistance issues associated with currently employed chemotherapeutics, LZ22 emerges as a promising candidate for adjunctive treatment in patients with malignant tumors.

Conclusion

In summary, this study presents compelling evidence that LZ22, a structurally novel small molecule compound isolated from *G. lucidum*, exerts a potent inhibitory effect on the growth, migration, and metastasis of tumor cells harboring wild-type p53 while exhibiting negligible efficacy against p53-deficient or mutant p53-expressing cells. The primary mechanism of LZ22 involves a high-affinity interaction with the histidine-96 pocket of the MDM2 protein, leading to the disruption of MDM2's binding to p53. This disruption is critical in preventing proteasomal degradation of p53. Furthermore, LZ22 restores the p53-dependent repression of CDK2/Rb signaling, effectively impeding cell cycle progression and reducing cell proliferation. Additionally, it relieves the p53-mediated repression of Snail expression and its downstream EMT, thereby significantly suppressing tumor cell migration and distal metastasis. Overall, our data reveal the antitumor activity and potential mechanisms of LZ22, providing new evidence for a comprehensive understanding of the anticancer activity of *G. lucidum* and offering a novel small-molecule agent for the treatment of malignancies.

Supporting Information

Supporting information of this paper can be requested by sending E-mails to the corresponding authors.

References

[1] Sung H, Ferlay J, Siegel RL, *et al*. Global cancer statistics 2020: GLOBOCAN estimates of incidence and mortality worldwide for 36 cancers in 185 countries [J]. *CA Cancer J Clin*, 2021, **71**(3): 209-249.

[2] Mehlen P, Puisieux A. Metastasis: a question of life or death [J]. *Nat Rev Cancer*, 2006, **6**(6): 449-458.

[3] Valastyan S, Weinberg RA. Tumor metastasis: molecular insights and evolving paradigms [J]. *Cell*, 2011, **147**(2): 275-292.

[4] Van't VLJ, Weigelt B. Road map to metastasis [J]. *Nat Med*, 2003, **9**(8): 999-1000.

[5] Wu Y, Wang Y, Lin Y, *et al*. Dub3 inhibition suppresses breast cancer invasion and metastasis by promoting Snail1 degradation [J]. *Nat Commun*, 2017, **8**: 14228.

[6] Steeg PS. Tumor metastasis: mechanistic insights and clinical challenges [J]. *Nat Med*, 2006, **12**(8): 895-904.

[7] Wang SP, Wang WL, Chang YL, *et al*. p53 controls cancer cell invasion by inducing the MDM2-mediated degradation of Slug [J]. *Nat Cell Biol*, 2009, **11**(6): 694-704.

[8] Chan SW, Tomlinson B, Chan P, *et al*. The beneficial effects of *Ganoderma lucidum* on cardiovascular and metabolic disease risk [J]. *Pharm Biol*, 2021, **59**(1): 1161-1171.

[9] Chang CJ, Lin CS, Lu CC, *et al*. *Ganoderma lucidum* reduces obesity in mice by modulating the composition of the gut microbiota [J]. *Nat Commun*, 2015, **6**: 7489.

[10] Geng X, Zhong D, Su L, *et al*. Preventive and therapeutic effect of *Ganoderma lucidum* on kidney injuries and diseases [J]. *Adv Pharmacol*, 2020, **87**: 257-276.

[11] Sohretoglu D, Huang S. *Ganoderma lucidum* polysaccharides as an anti-cancer agent [J]. *Anticancer Agents Med Chem*, 2018, **18**(5): 667-674.

[12] Levine AJ. p53: 800 million years of evolution and 40 years of discovery [J]. *Nat Rev Cancer*, 2020, **20**(8): 471-480.

[13] Prabhu VV, Allen JE, Hong B, *et al*. Therapeutic targeting of the p53 pathway in cancer stem cells [J]. *Expert Opin Ther Targets*, 2012, **16**(12): 1161-1174.

[14] Kim NH, Kim HS, Li XY, *et al*. A p53/miRNA-34 axis regulates Snail1-dependent cancer cell epithelial-mesenchymal transition [J]. *J Cell Biol*, 2011, **195**(3): 417-433.

[15] Muller PA, Vousden KH, Norman JC. p53 and its mutants in tumor cell migration and invasion [J]. *J Cell Biol*, 2011, **192**(2): 209-218.

[16] Zhou J, Kryczek I, Li S, *et al*. The ubiquitin ligase MDM2 sustains STAT5 stability to control T cell-mediated antitumor immunity [J]. *Nat Immunol*, 2021, **22**(4): 460-470.

[17] Haupt Y, Maya R, Kazaz A, *et al*. MDM2 promotes the rapid degradation of p53 [J]. *Nature*, 1997, **387**(6630): 296-299.

[18] Michael D, Oren M. The p53-MDM2 module and the ubiquitin system [J]. *Semin Cancer Biol*, 2003, **13**(1): 49-58.

[19] Wu X, Bayle JH, Olson D, *et al*. The p53-MDM-2 autoregulatory feedback loop [J]. *Genes Dev*, 1993, **7**(7A): 1126-1132.

[20] Juven-Gershon T, Oren M. MDM2: the ups and downs [J]. *Mol Med*, 1999, **5**(2): 71-83.

[21] Chène P. Inhibiting the p53-MDM2 interaction: an important target for cancer therapy [J]. *Nat Rev Cancer*, 2003, **3**(2): 102-109.

[22] Khoo KH, Verma CS, Lane DP. Drugging the p53 pathway: understanding the route to clinical efficacy [J]. *Nat Rev Drug Discov*, 2014, **13**(3): 217-236.

[23] Shangary S, Wang S. Small-molecule inhibitors of the MDM2-p53 protein-protein interaction to reactivate p53 function: a novel approach for cancer therapy [J]. *Annu Rev Pharmacol Toxicol*, 2009, **49**: 223-241.

[24] Li Y, Ren BX, Li HM, *et al*. Omeprazole suppresses aggressive cancer growth and metastasis in mice through promoting Snail degradation [J]. *Acta Pharmacol Sin*, 2022, **43**(7): 1816-1828.

[25] Ren BX, Li Y, Li HM, *et al*. The antibiotic drug trimethoprim suppresses tumor growth and metastasis *via* targeting Snail [J]. *Br J Pharmacol*, 2022, **179**(11): 2659-2677.

[26] Fu R, Han CF, Ni T, *et al*. A ZEB1/p53 signaling axis in stromal fibroblasts promotes mammary epithelial tumors [J]. *Nat Commun*, 2019, **10**: 3210.

[27] Pal S, Datta K, Mukhopadhyay D. Central role of p53 on regulation of vascular permeability factor/vascular endothelial growth factor (VPF/VEGF) expression in mammary carcinoma [J]. *Cancer Res*, 2001, **61**(18): 6952-6957.

[28] Santhanam U, Ray A, Sehgal PB. Repression of the interleukin 6 gene promoter by p53 and the retinoblastoma susceptibility gene product [J]. *Proc Natl Acad Sci U S A*, 1991, **88**(17): 7605-7609.

[29] Ueba T, Nosaka T, Takahashi JA, *et al*. Transcriptional regulation of basic fibroblast growth factor gene by p53 in human glioblastoma and hepatocellular carcinoma cells [J]. *Proc Natl Acad Sci U S A*, 1994, **91**(19): 9009-9013.

[30] Wade M, Li YC, Wahl GM. MDM2, MDMX and p53 in oncogenesis and cancer therapy [J]. *Nat Rev Cancer*, 2013, **13**(2): 83-96.

[31] Kussie PH, Gorina S, Marechal V, *et al*. Structure of the MDM2 oncoprotein bound to the p53 tumor suppressor transactivation domain [J]. *Science*, 1996, **274**(5289): 948-953.

[32] Suski JM, Braun M, Strmiska V, *et al*. Targeting cell-cycle machinery in cancer [J]. *Cancer Cell*, 2021, **39**(6): 759-778.

[33] Deng T, Yan G, Song X, *et al*. Deubiquitylation and stabilization of p21 by USP11 is critical for cell-cycle progression and DNA damage responses [J]. *Proc Natl Acad Sci U S A*, 2018, **115**(18): 4678-4683.

[34] Kortlever RM, Higgins PJ, Bernards R. Plasminogen activator inhibitor-1 is a critical downstream target of p53 in the induction of replicative senescence [J]. *Nat Cell Biol*, 2006, **8**(8): 877-884.

[35] Bieging KT, Mello SS, Attardi LD. Unravelling mechanisms of p53-mediated tumor suppression [J]. *Nat Rev Cancer*, 2014, **14**(5): 359-370.

[36] Duffy MJ, Synnott NC, McGowan PM, *et al*. p53 as a target for the treatment of cancer [J]. *Cancer Treat Rev*, 2014, **40**(10): 1153-1160.

[37] Engeland K. Cell cycle regulation: p53-p21-RB signaling [J]. *Cell Death Differ*, 2022, **29**(5): 946-960.

[38] Li Z, Razavi P, Li Q, *et al*. Loss of the FAT1 tumor suppressor promotes resistance to CDK4/6 inhibitors *via* the hippo pathway [J]. *Cancer Cell*, 2018, **34**(6): 893-905.e8.

[39] Freeman-Cook K, Hoffman RL, Miller N, *et al*. Expanding control of the tumor cell cycle with a CDK2/4/6 inhibitor [J]. *Cancer Cell*, 2021, **39**(10): 1404-1421.e11.

[40] Giaccone G. Clinical perspectives on platinum resistance [J]. *Drugs*, 2000, **59**(Suppl 4): 9-17.

[41] Köberle B, Tomicic MT, Usanova S, *et al*. Cisplatin resistance: preclinical findings and clinical implications [J]. *Biochim Biophys Acta*, 2010, **1806**(2): 172-182.

Cite this article as: REN Boxue, LI Yang, DI Lei, CHENG Ranran, LIU Lijuan, LI Hongmei, LI Yi, TANG Zhangrui, YAN Yongming, LU Tao, FU Rong, CHENG Yongxian, WU Zhaoqiu. A naturally derived small molecule compound suppresses tumor growth and metastasis in mice by relieving p53-dependent repression of CDK2/Rb signaling and the Snail-driven EMT [J]. *Chin J Nat Med*, 2024, **22**(2): 112-126.